JOURNAL OF CATALYSIS **140**, 173–183 (1993)

Electron Optical Studies of Fresh and Reduced Vanadium Pentoxide-Supported Rhodium Catalysts

A. LEGROURI,[1] T. BAIRD,[2] AND J. R. FRYER

Electron Microscope Centre, Chemistry Buildings, University of Glasgow, Glasgow G12 8QQ, United Kingdom

Received January 24, 1992; revised October 9, 1992

One percent Rh/V_2O_5 catalysts prepared by wet impregnation with $RhCl_3 \cdot xH_2O$ and subsequent reduction in hydrogen were shown to be subject to the formation of lower oxides of vanadium via an Rh-catalysed reduction process. V_4O_9, VO_2, and V_2O_3 compounds were observed at reduction temperatures of 250, 450, and 600°C, respectively, as characterised by IR, XRD, and electron optical methods. Maximum hydrogen uptake by the Rh-loaded V_2O_5 occurred at 155°C according to TPR data, and this contrasts with the onset of reduction of V_2O_5 alone at ~450°C. Mechanistic and structural aspects of the Rh-catalysed reduction process are discussed.

INTRODUCTION

Supported metal catalysts are widely employed in the chemical industry, with diverse applications such as petroleum refining, gas purification, and the treatment of vehicle exhaust emission. The traditional view considered the support as an inert carrier of the active component. More recent evidence, however, has established that with certain combinations of metals and supports the latter can influence the catalytic properties of the active component (*1*). The metal–support interaction effect may be defined as a direct influence of the support on the chemisorption and catalytic properties of the metal phase either by stabilising unusual metal particle structures, by changing the electronic properties due to electron transfer processes between the metal particles and the support, or by chemical bonding (compound formation) between metal and support (*2*).

The industrial importance of metal catalysts supported on reducible oxides, such as vanadium pentoxide, titania, and niobium oxide, has stimulated considerable research interest during the last few years (*3*); these supports are known to influence the active component by strong interaction (*2*). This article deals with the preparation and physicochemical characterisation of metallic Rh supported on V_2O_5 and with the observed catalytic reduction of the V_2O_5 support material at various temperatures. X-ray diffraction (XRD), infrared spectroscopy (IR), temperature-programmed reduction (TPR), scanning electron microscopy (SEM), and predominantly transmission electron microscopy (TEM) were employed in these studies. The latter technique provides particle size, size distribution, and metal dispersion data (*4, 5*) for comparison with other techniques such as chemisorption and XRD measurements which are essentially averaged data.

Several reviews have been the subject of the use of electron microscopy in supported metal catalyst characterisation (*6–12*).

EXPERIMENTAL

Materials

V_2O_5 powder was prepared by thermal decomposition of high purity ammonium

---

[1] Present address: Laboratoire de Chimie Physique, Faculté des Sciences Semlalia, Université Cadi Ayyad, B.P. S15, Marrakesh, Morocco.

[2] To whom correspondence should be addressed.

0021-9517/93 $5.00

metavanadate (Aldrich) at 400°C for 2 h under a stream of air (50 cm^3/min).

The metal loading of the catalyst was nominally 1% by weight Rh on V_2O_5 prepared by wet impregnating the support with the appropriate amount of an aqueous solution of $RhCl_3 \cdot xH_2O$ (Johnson Matthey).

Reduced samples of the metal-loaded catalyst and V_2O_5 itself were prepared by heating in a tubular furnace under a stream of hydrogen (50 cm^3/min) for 2 h at selected temperatures of 250, 450, and 600°C. After cooling, the samples were stored under vacuum in a desiccator prior to examination.

X-ray Diffraction

The XRD equipment used was a Philips diffractometer. The powdered samples were mounted flat on adhesive tape. They were rotated through 2θ angles of 3°–70° whilst being exposed to copper K_α radiation ($\lambda = 0.015418$ nm) at 40 kV and 20 mA. The resulting XRD patterns were recorded on a chart recorder operating at 400 counts per second.

Infrared Spectroscopy

The IR absorption spectra were registered on a Perkin–Elmer 580-B spectrophotometer. Samples were examined in the solid state in the form of thin discs containing approximately 2 mg of sample and 300 mg of spectroscopic potassium bromide (BDH). Spectra were recorded in the range 4000 to 250 cm^{-1}.

Transmission Electron Microscopy

Suitably thin samples for examination by TEM were prepared ultrasonically from suspensions in water or ethanol. Specimens were mounted on standard 3-mm copper grids covered with a carbon film. Observations were made with a JEOL 1200EX electron microscope. The TEM magnification was calibrated using 0.335-nm fringes from graphite present on the sample grids.

An optical bench was normally used to measure the lattice spacings observed in the HREM images. A grating of known spacing was used as a standard.

Scanning Electron Microscopy

SEM was undertaken with a Philips 501B instrument operated at 15 kV. Samples were mounted separately on aluminium stubs and precoated with gold in a sputter coater to minimise the severe charging effects that proved to be characteristic of these materials.

Temperature-Programmed Reduction

In our apparatus a gas mixture (6% hydrogen–94% nitrogen), with a flow rate of 20 cm^3/min, can be directed through a microreactor, containing the catalyst, which is surrounded by a cylindrical furnace. The temperature of the furnace was controlled by a linear temperature programmer (Stanton Redcroft LVP/CA 40/R). The catalyst was heated linearly at a rate of 5°C/min. Hydrogen consumption was monitored continuously by means of a thermal conductivity detector.

RESULTS AND DISCUSSION

Structural Characterisation of Fresh and Reduced Rh/V_2O_5 Catalysts

X-ray diffraction. XRD showed that the fresh catalyst support material was crystalline, diffraction data (Fig. 1) being in good agreement with those of pure V_2O_5 (*13–15*). Reduction of the catalyst in hydrogen at 250°C gave *d*-spacings (Fig. 1) for both V_2O_5 and V_4O_9 (*16*). The relative intensities of the peaks indicated that the support was predominantly V_4O_9 at 250°C. Further reduction to VO_2 (*17*, *18*) occurred at 450°C, and at 600°C XRD data indicated the formation of either V_2O_3 (*19*) or VO (*20*), which have similar *d*-spacings. Subsequent TEM results indicated the former compound was formed.

The low metal loading (1% by weight) did not permit XRD data to be observed for the Rh component, as expected.

In contrast, no reduction of V_2O_5 was in-

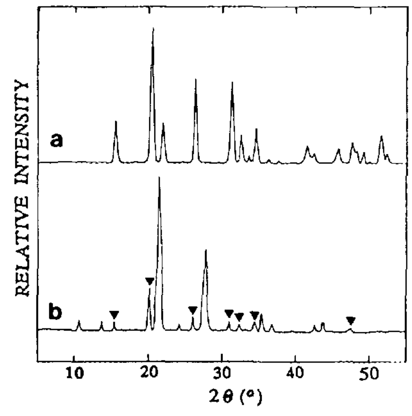

FIG. 1. XRD patterns corresponding to (a) V_2O_5 for the fresh catalyst and (b) a mixture of V_2O_5 (▼) and V_4O_9 for the catalyst reduced at 250°C.

dicated by XRD within detectable limits (~5% by weight) when pure V_2O_5 was treated with hydrogen under the same conditions, thus implying a catalytic influence of Rh on the reduction process.

Infrared spectroscopy. The IR spectrum exhibited by the fresh catalyst (Fig. 2) corresponded to that found for pure V_2O_5 (*21*, *22*). Typical for this compound are the high-frequency bands at 1020 and 995 cm^{-1} which were attributed to the stretching vibration of unshared V=O bonds. Reduction at 250° gave absorptions for V_4O_9 and possibly V_2O_5. Typical of V_4O_9 (*23*, *24*) is the band at 920–930 cm^{-1} composed of several sharp peaks. Common structural features of V_4O_9 and V_2O_5 give rise to similarities in their spectra. The considerable weakening of the high-frequency bands after reduction can be explained by the fact that the oxygen atoms of the vanadyl groups are the most affected in the reduction process. After reduction at 450°C, the spectrum developed bands consistent with vanadium dioxide, VO_2 (*25*, *26*). The broad band at ~670 cm^{-1} has been attributed to V–O–V stretching vibrations (*26*). Reduction at 600°C produced some new bands, especially below 800 cm^{-1}, and these remain unassigned.

Electron optical studies. The gross morphological changes occurring in the V_2O_5 on progressive reduction were clearly manifested by the SEM studies. The fresh catalyst consisted of well-formed crystals with smooth faces and sharp edges (Fig. 3a). Cracks developed at higher temperatures with increasing severity (e.g. Fig. 3b at 450°C), owing to the mass loss of oxygen from the V_2O_5 and the structural rearrangement to the lower oxides. Despite the severe shrinkage observed, the overall integrity of the original crystalline masses was retained.

High-resolution TEM images and electron diffraction patterns of the various catalysts yielded lattice images and electron diffraction data consistent with the corresponding support phases characterised by XRD and IR at each temperature. Representative electron micrographs are shown

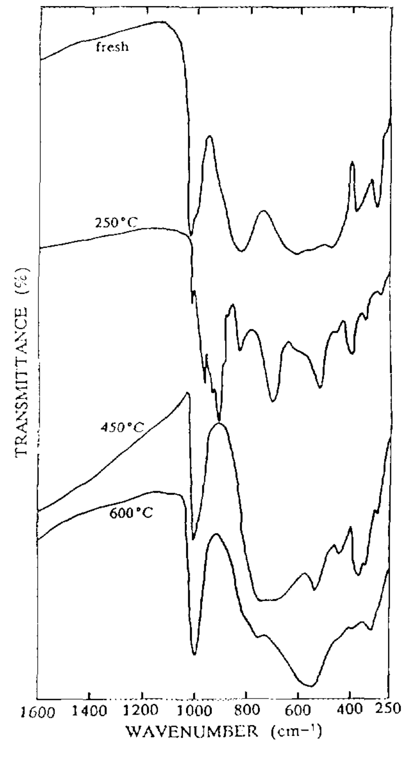

FIG. 2. IR spectra of the fresh catalyst and after reduction at 250, 450, and 600°C.

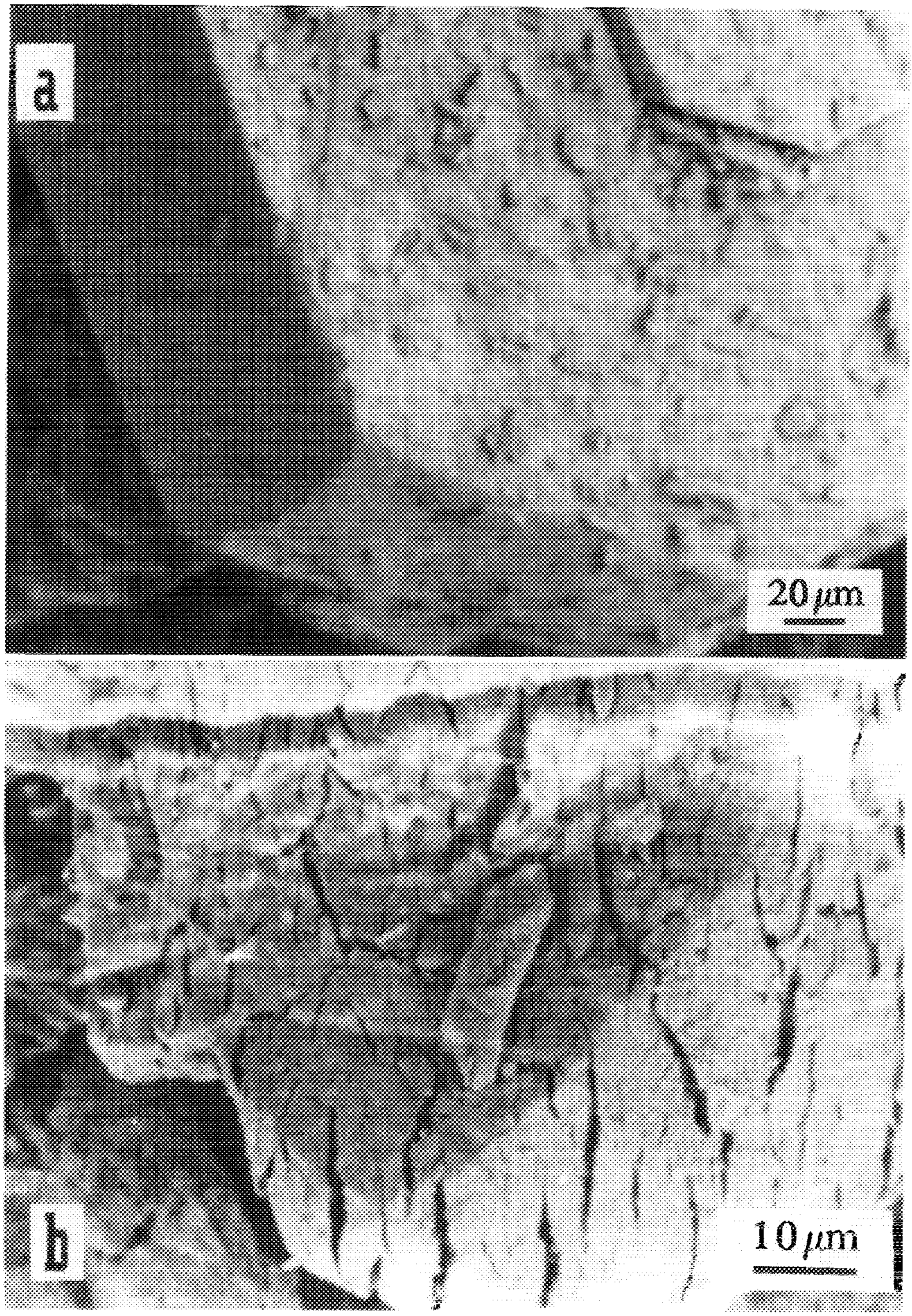

Fig. 3. Scanning electron micrographs of (a) the fresh catalyst (b) a catalyst reduced at 450°C showing crack formation.

in Fig. 4. The 0.58-nm and 0.34-nm lattices in Fig. 4a are typical of V_2O_5 unreduced. Reduction at 250°C gave lattices (Fig. 4b) in accord with V_4O_9 mainly but with some V_2O_5 lattices also present. The reflections in the diffraction pattern in Fig. 4b are in agreement with the orientation of crystallographic planes in the tetragonal structure described by Theobald *et al.* (*16*) for V_4O_9. The measured angles of 52° and 38° between the (011) and (002) planes and the (011) and (020) planes are close to the calculated values of 51.4° and 38.6° for a tetragonal unit cell. The data also fit with the orthorhombic structure favoured by Grymonprez *et al.* (*27*), in which case the planes would be indexed as (012), (020), and (004) instead of (011), (002), and (020) as given above for a tetragonal cell. Catalysts reduced at 450°C provided lattice images and electron diffraction patterns that corresponded with VO_2 (Fig. 4c). Reduction at 600°C gave data (Fig. 4d) that were in agreement with V_2O_3 (*19*) rather than VO (*28*, *29*), for example, the 0.365-nm lattices corresponding to the (102) planes of V_2O_3.

Metallic particles of Rh were also observed on the support for reduced samples, for example, as shown in Fig. 5. The particles exhibited different shapes and sizes. The particle size distributions at each reduction temperature measured from about 1000 particles are given in Fig. 6. The average particle diameters were found to be 4.1, 5.2, and 6.5 nm for catalysts reduced at 250, 450, and 600°C, respectively. It is evident that the thermal treatment has caused particle sintering. The single CO chemisorption experiment on the 250°C reduced catalyst yielded an average particle diameter of 3.8 nm, which is close to the TEM result (4.1 nm).

The Rh-Catalysed Reduction of V_2O_5

Temperature-programmed reduction. The TPR trace of the fresh catalyst up to 500°C (Fig. 7a) showed one distinct peak with a maximum at 155°C. The uptake of hydrogen corresponding to this reduction was measured to be 0.0365 dm^3/g of catalyst. The theoretical amount necessary for the reduction of all Rh to the metallic state, if it existed as Rh^{3+} before reaction, is calculated to be 0.00326 dm^3/g of catalyst and indicates that most of the hydrogen taken up was used for support reduction. Complete reduction to V_4O_9 would require 0.064 dm^3/g of catalyst, and thus partial reduction (~50%) is inferred. The reduction of Rh ions supported on nonreducible oxides such as alumina and silica, by comparison, was found to occur at the higher temperatures of 167 and 178°C, respectively (*30*).

When pure V_2O_5 was heated in hydrogen up to 700°C, the onset of reduction was not observed until ~450°C (Fig. 7b) with continuous uptake up to 700°C. Reported TPR spectra for pure V_2O_5 differ from the present results. Roozeboom *et al.* (*31*) found a single reduction peak at ~527°C. At higher temperatures, Bosch *et al.* (*32*) found two peaks with maxima at 650 and 690°C, and they suggested that the reduction of V_2O_5 proceeded via V_6O_{13} to VO_2. It is difficult to compare directly TPR data obtained by different investigators, since the experimental conditions differ widely in hydrogen concentration, flow rate, sample size, and pretreatment. The present results clearly show, however, in agreement with the XRD, IR, and TEM results, that the presence of Rh catalyses the reduction of V_2O_5.

Mechanistic viewpoints on the Rh-cata-

FIG. 4. High-resolution electron micrographs of (a) fresh catalyst with 0.58-nm and 0.34-nm lattice fringes of V_2O_5, (b) catalyst reduced at 250°C with 0.643-nm (011) and 0.520-nm (002) lattices of V_4O_9 (inset electron diffraction pattern of V_4O_9), (c) catalyst reduced at 450°C with 0.32-nm (011) lattices for VO_2 (inset EDP of VO_2), and (d) catalyst reduced at 600°C with 0.365-nm lattices for V_2O_3.

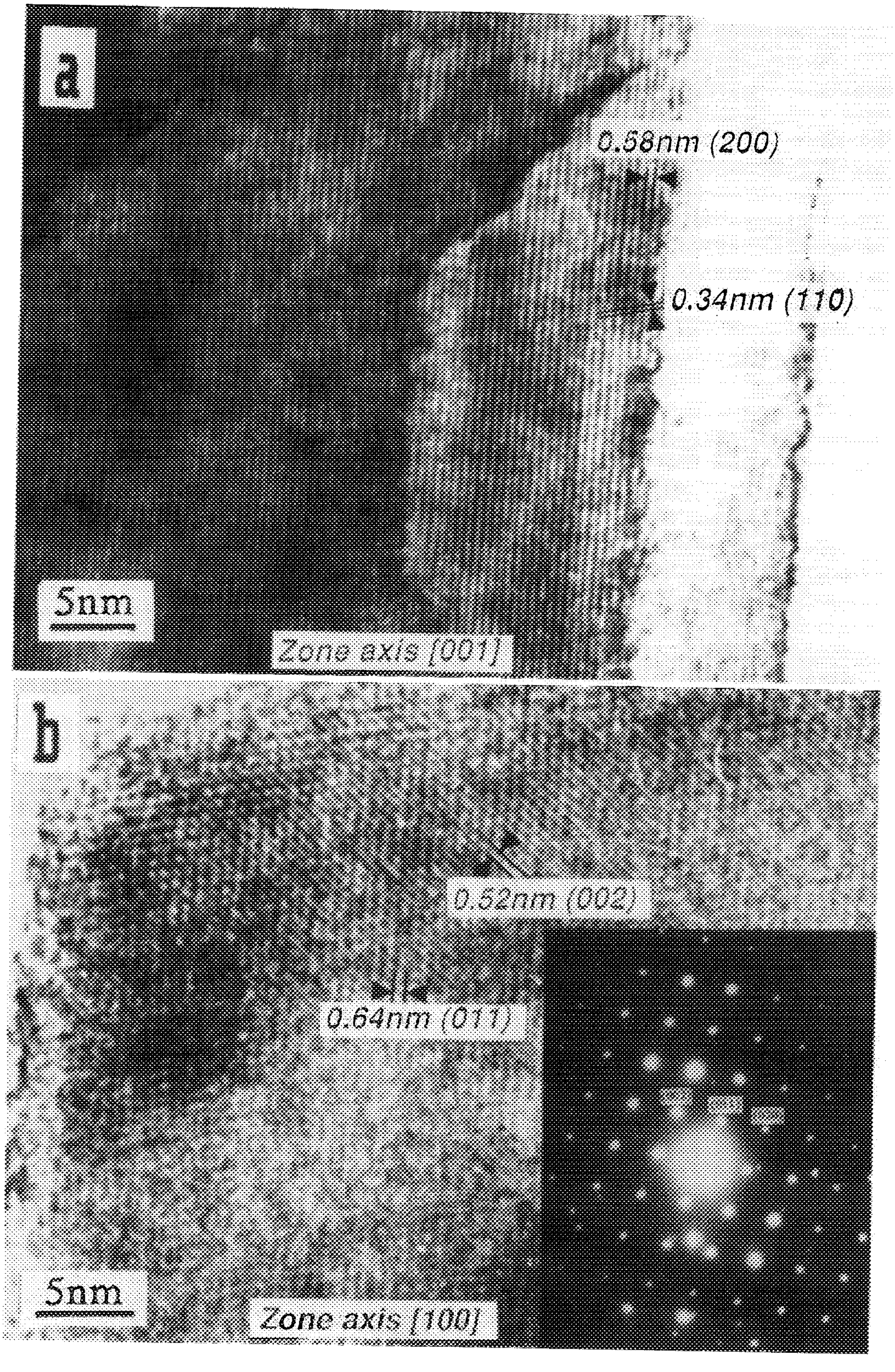
a
0.58nm (200)
0.34nm (110)
5nm
Zone axis [001]
b
0.52nm (002)
0.64nm (011)
5nm
Zone axis [100]

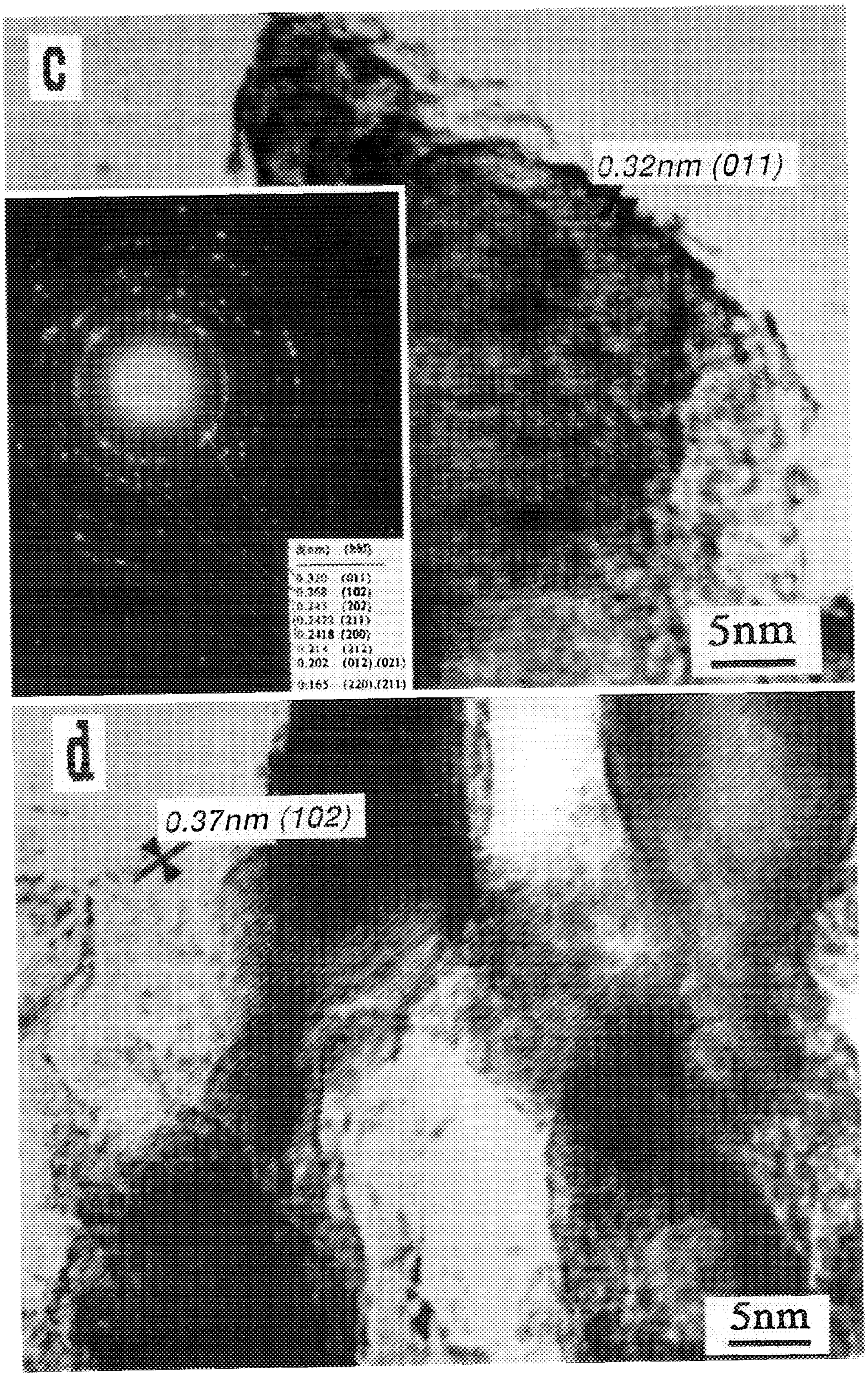
c
0.32nm (011)
d(nm) (hkl)
0.329 (011)
0.368 (102)
0.243 (202)
0.2422 (211)
0.2418 (200)
0.214 (212)
0.202 (012),(021)
0.165 (220),(211)
5nm
d
0.37nm (102)
5nm

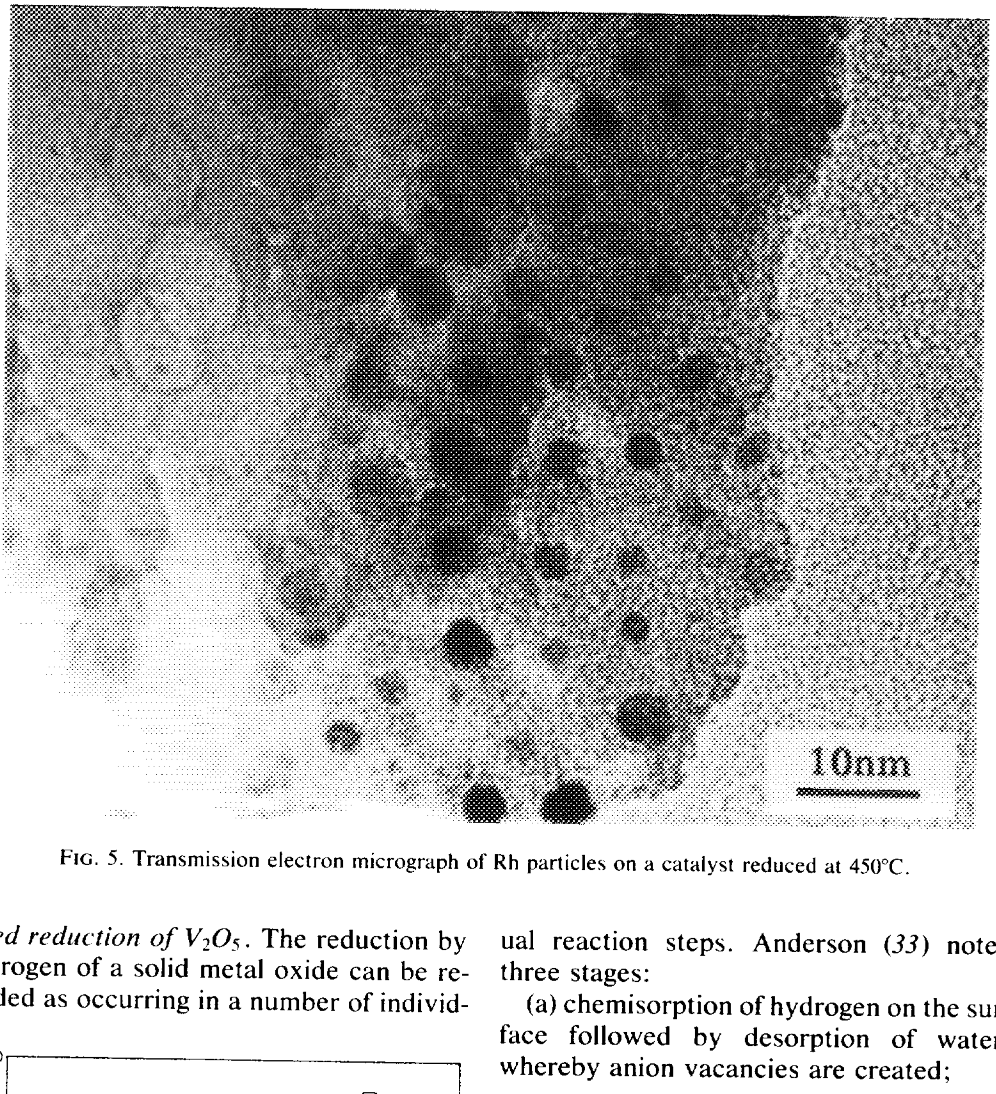

FIG. 5. Transmission electron micrograph of Rh particles on a catalyst reduced at 450°C.

lysed reduction of V_2O_5. The reduction by hydrogen of a solid metal oxide can be regarded as occurring in a number of individual reaction steps. Anderson (*33*) noted three stages:

(a) chemisorption of hydrogen on the surface followed by desorption of water, whereby anion vacancies are created;

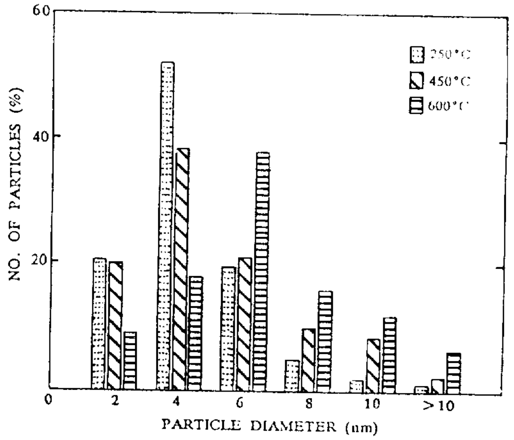

FIG. 6. Histograms of Rh particle size distributions for catalysts reduced at 250, 450, and 600°C.

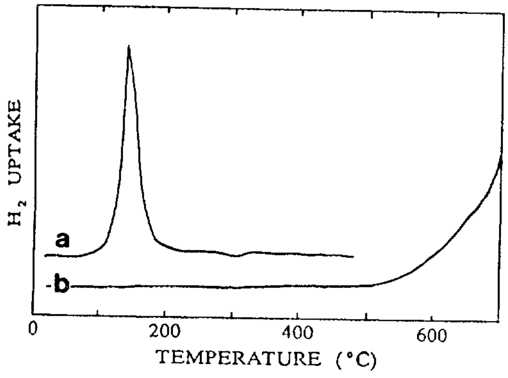

FIG. 7. TPR traces for (a) fresh (Rh-loaded) catalyst and (b) V_2O_5 alone.

(b) diffusion of the vacancies from the surface into the bulk;

(c) saturation of the crystal lattice with defects followed by nucleation of the new phase.

The above scheme probably applies to the reduction of the metal-free V_2O_5 in the present work.

One of the effects of the close interaction between metal and support in supported metal catalysts is the phenomenon of hydrogen spillover (*34, 35*). Since hydrogen is activated on the surface of the supported crystallites, the points of contact between them and the oxide being reduced become centres for rapid production and growth of nuclei of the new phase. As a result, there is a sharp decrease in the duration of the induction period and a change in the kinetics of nucleus formation. Such effects undoubtedly account for the enhanced reduction of V_2O_5 in the presence of Rh in the present studies.

It is widely accepted that the migration of hydrogen atoms from the activating species to the acceptor is the initiating step (*36*). The first hydrogen atoms to arrive on the oxide surface are thought to react as

$$M^{n+} + O^{2-} + H \rightarrow M^{(n-1)+} + OH^-,$$

and that this is followed by dehydration to the next lower oxide. Such a reaction scheme explains the stepwise reduction of V_2O_5 and explains why V_4O_9 is the first product observed and not VO_2 or V_2O_3.

The Rh salt precursor, prior to reduction, was believed to exist in a highly dispersed form over the surface of the V_2O_5 crystals, as no evidence for it was observed on TEM examination. Rh particles were seen to have formed in all subsequent samples reduced in hydrogen.

TEM examination of the Rh-loaded catalysts revealed an increased mass loss resulting in hole formation (voids) in the oxide with increasing reduction temperature. In general, the holes produced did not appear to be associated with Rh particles and there was no evidence of channeling by catalyst particles (Fig. 8). The holes probably result from the initiation of the reduction process by migrating hydrogen atoms formed on the metal surface, with subsequent local atomic rearrangement at active sites in the oxide. Generally, there was no relationship between the edges of the holes and crystallographic planes of the reduced oxide, although occasionally there were exceptions.

Crystal structure changes occurring on reduction of vanadium oxides. V_2O_5 can be considered to be composed of an alternate succession of oxygen atom planes and vanadium–oxygen atom planes (Fig. 9). The transformation from V_2O_5 to lower oxides requires the elimination of specific oxygen atoms. It has been shown (*37*) that the removal of all oxygen atoms indicated by arrows in Fig. 9 will lead to the monoclinic structure of V_6O_{13} (*38*) after atomic rearrangement (Fig. 10). The formation of V_6O_{13} would thus require the elimination of every third oxygen plane. Lower oxides of vanadium may form by a similar process. Removal of every second plane would lead to VO_2, and elimination of all the oxygen planes would give V_2O_3. The fact that V_4O_9 was observed to grow topotactically on V_2O_5 single crystals, i.e., with 1/10 of the oxygen atoms removed from the V_2O_5 structure, together with other considerations, led Grymonprez *et al.* (*27*) to the view that V_4O_9 could be thought of as a slightly deformed superstructure of V_2O_5; these authors (*27*) discuss V_2O_5/V_4O_9 superstructure relationships and they suggest that the slight differences between them could be accommodated by minor distortions, the driving force for which could be the repulsive action between oxygen vacancies. The vanadyl oxygen atoms in V_2O_5 appear to be the most reactive (*39*) and are thus likely to be the ones most easily removed on reduction. The observed diminution of the high-frequency IR bands attributed to vanadyl groups in the present work is in keeping with an enhanced reactivity for unshared VO groups.

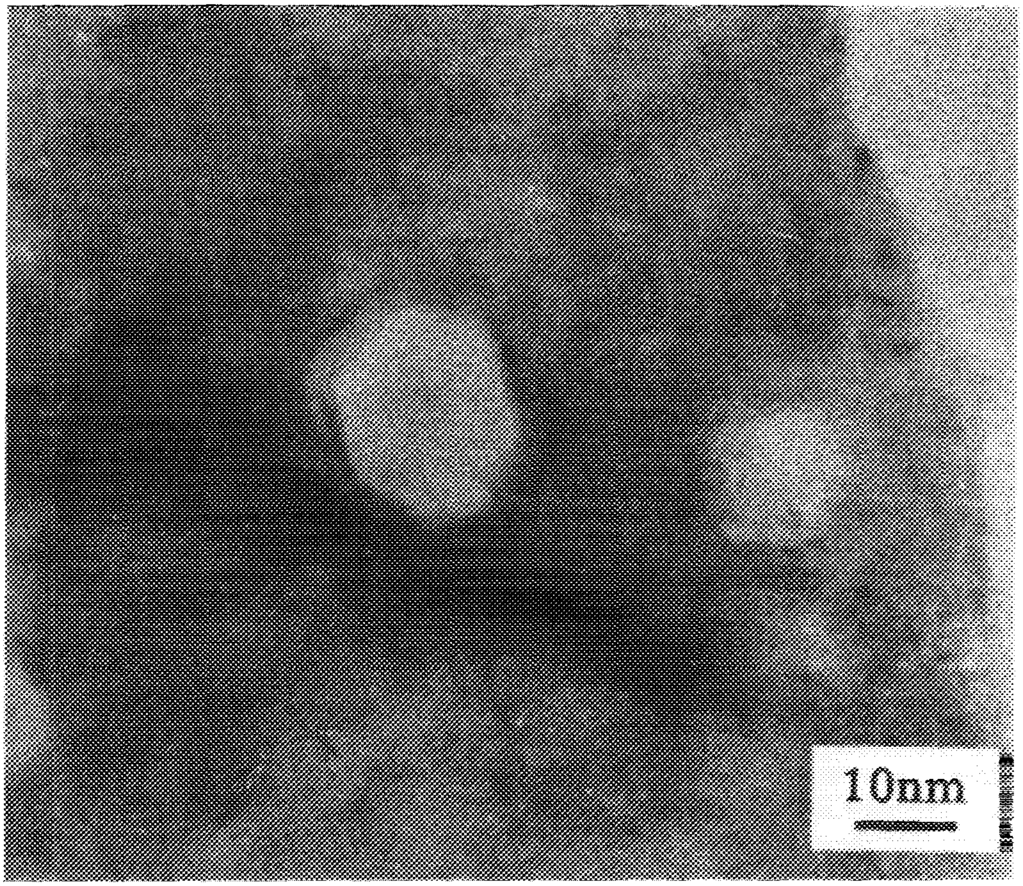

FIG. 8. High-resolution electron micrograph showing hole formation in a reduced catalyst (250°C). The edges of the larger pseudo-hexagonal hole appear to be parallel to V_4O_9 lattice fringes (exceptional case).

CONCLUSIONS

(i) 1% Rh/V_2O_5 catalysts were characterised mainly by electron optical, XRD, IR, and TPR methods.

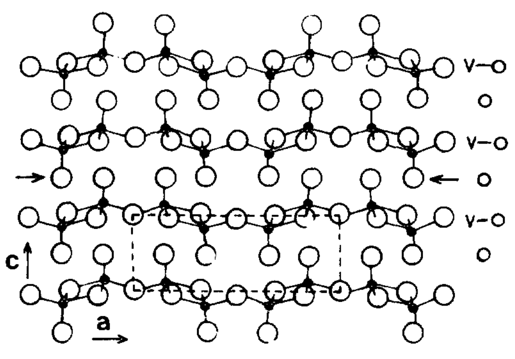

FIG. 9. Projection of V_2O_5 structure on to the (010) plane.

(ii) The data obtained by the various techniques were in good agreement with each other and showed that V_2O_5 loaded with 1% Rh was catalytically reduced in a stepwise manner via V_4O_9, VO_2, and V_2O_3 at 250, 450, and 600°C, respectively.

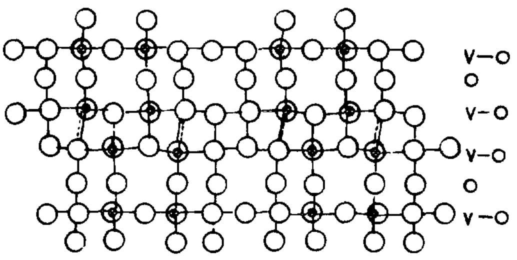

FIG. 10. Projection of V_6O_{13} structure on to the (010) plane.

(iii) In the absence of Rh particles the onset of reduction by hydrogen occurred at ~450°C, as shown by TPR measurements. In contrast, Rh-loaded V_2O_5 exhibited maximum uptake of hydrogen at 155°C.

(iv) SEM and TEM studies revealed the structural features that occurred on reduction of the catalysts, including metal particle sintering and void formation.

(v) Mechanistic and structural aspects of the catalysts were discussed.

ACKNOWLEDGMENTS

We thank the SERC for funding towards the provision of electron microscopes and the British Council for a TCT Award for A. Legrouri.

REFERENCES

1. Bond, G. C., and Burch, R., *in* "Catalysis 'Spec. Period Rep.'" (G. C. Bond and G. Webb, Eds.), Vol. 6, p. 27. Roy. Soc. Chem., London, 1983.
2. Imelik, B., Naccache, C., Coudurier, G., Praliaud, H., Mériaudeau, P., Gallezot, P., Martin, G. A., and Védrine, J. C. (Eds.), "Metal-Support and Metal-additive Effects in Catalysis." Elsevier, Amsterdam, 1982.
3. Foger, K., *in* "Catalysis-Science and Technology" (J. R. Anderson and M. Boudart, Eds.), Vol. 6, p. 227. Springer-Verlag, Berlin, 1984.
4. Prestridge, E. B., and Yates, D. C. J., *Nature (London)* **234,** 345 (1971).
5. Nakamura, M., Yamada, M., and Amano, A., *J. Catal.* **39,** 125 (1975).
6. Howie, A. *in* "Characterisation of Catalysts" (J. M. Thomas and R. M. Lambert, Eds.), p. 89. Wiley, Chichester, 1980.
7. Poppa, H., and Heinemann, K., *Optik (Stuttgart)* **56,** 183 (1980).
8. Baird, T., "Catalysis 'Spec. Period Rep.'" (G. C. Bond and G. Webb, Eds.), Vol. 5, p. 172. Roy. Soc. Chem., London, 1982.
9. Baird, T., *in* "Electron Microscopy and Analysis" (P. Doig, Ed.), Institute of Physics Conference Series, No. 68 p. 239. Taylor and Francis, New York, 1983.
10. Yacaman, M. J., *Appl. Catal.* **13,** 1 (1984).
11. Sanders, J. V., *in* "Catalysis-Science and Technology" (J. R. Anderson and M. Boudart, Eds.), Vol. 7, p. 51. Springer-Verlag, Berlin, 1985.
12. Matyi, R. J., Schwartz, L. H., and Butt, J. B., *Catal Rev. Sci. Eng.* **29,** 41 (1987).
13. File No. 9-387, *Nat. Bur. Stand.* Circ. (*U.S.*) **539** (8), 66 (1958).
14. Enjalbert, R., and Galy, J., *Acta Crystallogr. Sect. C* **42,** 1467 (1986).
15. Legrouri, A., Baird, T., and Fryer, J. R., *React. Solids* **5,** 53 (1988).
16. Theobald, F., Cabala, R., and Bernard, J., *C.R. Acad. Sci. Paris, Ser. C* **269,** 1209 (1969).
17. Andersson, G., *Acta Chem. Scand.* **8,** 1599 (1954).
18. Longo, J. M., and Kierkegaard, P., *Acta Chem. Scand.* **24,** 420 (1970).
19. File No. 1-1293, Inorganic index to the powder diffraction file, Acta Philadelphia: Joint Committee on Powder Diffraction Standards.
20. Mukherjee, A., *J. Less-Common Met.* **107,** 89 (1985).
21. Abello, L., Husson, E., Repelin, Y., and Lucazeau, G., *Spectrochim. Acta Part A* **39,** 641 (1983).
22. Clauws, P., Broeckx, J., and Vennik, J., *Phys. Status Solidi B* **131,** 459 (1985).
23. Theobald, F., *Rev. Roum. Chim.* **23,** 887 (1978).
24. Clauws, P. *Verh. K. Acad. Wet. Lett. Schone Kunsten Belg. Kl. Wet.* **42,** 159 (1980).
25. Kimizuka, N., Ishii, M., Kawada, I., Saeki, M., and Nakahira, M., *J. Solid State Chem.* **9,** 69 (1974).
26. Pereleyev, V. A., Miller, V. I., Perelyaeva, L. A., Grebenshchikova, N. E., Shveikin, G. P., and Chirkov, A. K., *Russ. J. Inorg. Chem.* **22,** 1267 (1977).
27. Grymonprez, G., Fiermans, L., and Vennik, J., *Acta Crystallogr. Sect. A* **33,** 834 (1977).
28. Anderson, J. S., *in* "Defects and Transport in Oxides" (M. S. Seltzer and R. I. Jaffee, Eds.), p. 30. Plenum, New York, 1974.
29. Smith, D. J., McCartney, M. R., and Bursill, L. A., *Ultramicroscopy* **23,** 299 (1987).
30. Boumarafi, B., M.Sc. Thesis, Glasgow Univ., 1986.
31. Roozeboom, F., Mittelmeyer-Hazeleger, M. C., Moulijn, J. A., Medema, J., de Beer, V. H. J., and Gellings, P. J., *J. Phys. Chem.* **84,** 1783 (1980).
32. Bosch, H., Kip, B. J., van Ommen, J. G., and Gellings, P. J., *J. Chem. Soc. Faraday Trans. 1* **80,** 2479 (1984).
33. Anderson, J. S., *Discuss Faraday Soc.* **4,** 163 (1948).
34. Khoobiar, S. J., *J. Phys. Chem.* **68,** 411 (1964).
35. Sermon, P. A., and Bond, G. C., *Catal Rev.* **8,** 211 (1973).
36. Bond, G. C., and Tripathi, J. B. P., *J. Chem. Soc. Faraday Trans 1* **72,** 933 (1976).
37. Gillis, E., *C.R. Acad. Sci. Paris* **258,** 4765 (1964).
38. Aebi, F., *Helv. Chim. Acta* **31,** 8 (1948).
39. Tarama, B. K., Teranishi, S., Yoshida, S., and Tamura, T., *in* "Proceedings, 3rd International Congress on Catalysis, Amsterdam, 1964" (W. M. H. Sachtler, G. C. A.. Schuit, and P. Zwietering, Eds.), Vol. 1, p. 282. North-Holland, Amsterdam, 1965.